Appl. Phys. A (2015) 119:497–502
DOI 10.1007/s00339-014-8980-4

Applied Physics A
Materials Science & Processing

Polyol thermolysis synthesis of TiO_2 nanoparticles and its paste formulation to fabricate photoanode for dye-sensitized solar cells

P. Pratheep · E. Vijayakumar · A. Subramania

Received: 28 October 2014 / Accepted: 31 December 2014 / Published online: 13 January 2015

Abstract Titanium dioxide (TiO_2) nanoparticles (NPs) were prepared by a simple polyol thermolysis process using various mole ratios of titanium tetrachloride ($TiCl_4$) and polyvinylpyrrolidone (PVP). The prepared TiO_2 NPs were characterized by TG/DTA, XRD, SEM, and BET analysis. The TiO_2 NPs obtained using 0.1 M of $TiCl_4$ and 0.02 M of PVP have high surface area with lesser particles size than the same obtained using 0.1 M of $TiCl_4$ with other mole ratios of PVP. The high surface area TiO_2 NPs were used to formulate TiO_2 paste. The impact of ethyl cellulose, terpineol, and dibutyl phthalate in the formulation of TiO_2 paste was optimized with respect to standard TiO_2 paste (*Dyesol Ltd.*) on the adsorption of dye was studied by UV–Vis spectroscopy. The photovoltaic performance of DSSCs fabricated using the formulated TiO_2 paste has achieved 97.83 % of power conversion efficiency (PCE) ($\eta = 4.5$ %) with respect to the standard TiO_2 paste (*Dyesol Ltd.*) and its PCE were found to be 4.6 % (η). This PCE value was nearly closer to that of the same DSSC fabricated using the standard TiO_2 paste (*Dyesol Ltd.*) and higher than the P25 TiO_2 (*Degussa*) paste and its achieved PCE were found to be 86.04 %.

1 Introduction

Dye-sensitized solar cells (DSSCs) are considered as one of the most promising type of photovoltaic cell developed in the recent years due to their relatively inexpensive manufacturing cost [1]. The high surface area photoanode and quantity of dye adsorbed on the photoanode are the key components for achieving high PCE [2]. The PCE also depends strong on the surface and electronic properties of nanocrystalline TiO_2 film. The chemicals used to formulate the TiO_2 paste influence the properties of nanocrystalline TiO_2 film. The NPs distribution, crack-free surface, interconnectivity of the NPs, and adhesion of the film are important physical parameters that also affect the efficiency of the DSSCs [2–4]. Hence, it is essential to prepare TiO_2 NPs with high surface area and also to optimize the chemical formulation while preparing TiO_2 paste to get inter connected, uniformly distributed NPs with crack-free surface for the fabrication of DSSCs. Methods of synthesis of TiO_2 play a vital role to fulfill the requirements like sol–gel, microwave assisted, hydrothermal, simple polymer technique, polyol thermolysis, and many others [5–9]. Among these methods, polyol thermolysis method is very easy and low-cost method for preparing metal oxide nanoparticles with uniform size distribution. In this method, high boiling point polyol is used to act as a stabilizer, limiting the particles growth and also prohibiting the agglomeration of the particles due to the formation of highly crystalline oxides [11]. At the very first, our group has synthesized MgO NPs via PTP [11]. Jungwon et al. [9] have prepared the TiO_2 NPs using a mixture of titanium isopropoxide and triethylene glycol. Suraj et al. [12] have also prepared the TiO_2 NPs from a mixture of titanium isopropoxide and ethylene glycol. In addition, PVP is used as a capping agent and it has a significant effect on the formation of nanoparticles of uniform size distribution without any agglomeration during the synthesis [11].

In the present investigation, we prepared TiO_2 NPs from polyol thermolysis process by varying the mole ratios of $TiCl_4$ and PVP to get uniform particle size with high

P. Pratheep · E. Vijayakumar · A. Subramania (✉)
Electrochemical Energy Research Lab, Centre for Nanoscience and Technology, Pondicherry University, Pondicherry 605 014, India
e-mail: a.subramania@gmail.com

surface area. This was used to prepare TiO_2 paste by using an optimized chemical formulation. This TiO_2 paste was used to fabricate TiO_2 photoanode, and its influence on the adsorption of dye and PCE was discussed in detail.

2 Experimental part

2.1 Materials

Titanium tetrachloride (99.0 % Sigma-Aldrich), polyvinylpyrrolidone (PVP, Aldrich), ethylene glycol (EG, Merck) were used for the preparation of TiO_2 NPs. Ethyl cellulose (EC, Ottokemi), terpineol (Himedia), dibutyl phthalate (Merck) were used for the preparation of TiO_2 paste.

2.2 Synthesis of TiO_2 NPs

TiO_2 NPs were synthesized by polyol thermolysis process using the following procedure: 0.1 mol of titanium tetrachloride and various mole ratios of PVP were taken in round bottom flasks and then dissolved in EG. They were refluxed at ~195 °C for 2 h, where the light yellow color solution turned to form white flocculate. The NPs were collected from the solutions by centrifugation at 6,000 rpm at room temperature. The excess amount of physically adsorbed PVP and EG on white flocculates was removed by washing with deionized water and ethanol for several times. The resultant samples were dried in a vacuum oven at 80 °C for 2 h, and then, the collected samples were annealed at 500 °C in air for 2 h to form TiO_2 NPs with improved quality [11].

2.3 Characterization of TiO_2 NPs

Thermogravimetric analysis (TGA) and differential thermal analysis (DTA) of the prepared TiO_2 were carried out (TA Instrument, Model: Q600 SDT) at the heating rate of 10 °C/min up to 600 °C. The phase purity of the products was examined by X-ray diffraction analysis (Rigaku Ultima-IV) using Cu–K_α radiation source with the scan rate of 0.02° per second. The band gap determination and dye adsorption of the prepared TiO_2 were studied by UV–Vis spectrometer (Perkin Elmer spectrometer). The surface morphology of the prepared TiO_2 was studied by SEM analysis (Hitachi, Model: S-3400N). The specific surface area of TiO_2 NPs obtained from various mole ratios of PVP was measured by BET method using N_2 adsorption (Micromeritics, Model: Gemini 2390-t).

2.4 Formulation of TiO_2 paste

The photoanode paste was prepared by mixing an optimized amount of 30 wt% prepared TiO_2 NPs (using 0.02 M PVP) along with 15 wt% of ethyl cellulose (binder), 50 wt% of terpineol (solvent) and 5 wt% of dibutyl phthalate (plasticizer). It was then stirred well followed by intermittent sonication to get TiO_2 paste.

2.5 Fabrication of DSSCs

The FTO glass plates were first cleaned in a detergent solution for 5 min using an ultrasonic bath, followed by cleaning in deionized water and 1:1 (v/v) mixture of ethanol and acetone-containing solvent for ultrasonic cleaning at about 5 min and then dried in air. The prepared TiO_2 paste and standard TiO_2 paste (*Dyesol Ltd.*) were coated on each FTO glass plate by the doctor-blade technique. The thickness of the films was found to be around 10–12 μm. The area of the photoanodes was 0.20 cm^2. They were sintered at 450 °C in a muffle furnace at 5 °C/min for 30 min to remove the organic ingredients to facilitate the interconnection among the TiO_2 NPs. After cooling to 80 °C, the TiO_2 electrodes were immersed into the purified N719 dye solution for 24 h at 30 °C. The standard Pt paste (*Dyesol Ltd.*) was coated on FTO glass plates, followed by sintering in a muffle furnace at 450 °C for 30 min. Finally, each photoanodes and counter electrodes were sandwiched with thermal adhesive films (Surlyn, Dupont 1702, 60 μm-thick) by a hot press to avoid the short-circuiting of the cell [13]. The electrolyte, 0.5 M 1-butyl-3-methylimidazolium iodide, 0.5 M LiI, 0.05 M I_2, 0.5 M 4-tert-butylpyridine in acetonitrile, was poured into the holes, drilled in the counter electrode, and then sealed with small squares of surlyn strip [14].

2.6 Photovoltaic performance of DSSCs

DSSCs were fabricated using the formulated TiO_2 paste (0.02 M PVP)-based photoanode, and their photovoltaic performance was studied by AM 1.5 solar simulator (Newport, Oriel Instruments, USA 150 W; Model: 67005) with a light intensity of 100 mW/cm^2 calibrated using a standard mono-crystalline silicon solar cell (Newport, Oriel Instruments, Model: 91150V) and a computer-controlled digital source meter (Keithley, Model: 2420). This result was compared with that of the same DSSC fabricated using a standard TiO_2 paste (*Dyesol Ltd.*)-based photoanode. We fabricated three DSSCs for each system and their photovoltaic values were measured and average values were taken.

3 Results and discussion

3.1 Thermal studies

The simultaneous TG and DTA curves of the TiO_2 precursor are depicted in Fig. 1. As the temperature increased

from 30 to 100 °C, a small weight loss of ~17 % was observed due to loss of moisture and organic impurities in the precursor. It is evident from the DTA curve which showed a long endothermic peak at ~90 °C. Again an exothermic peak appeared at 340 °C by increasing the temperature from 100 to 340 °C, and a gradual weight loss of ~15 % was observed due to the decomposition of the side chain of PVP as well as the low-molecular weight organic matter. Subsequently, a steep slope indicates the huge weight loss of PVP to complete decomposition up to 475 °C. Beyond 475 °C, no decomposition appeared. This suggests that the decomposition completed at 475 °C and the pure anatase TiO_2 remain at the temperature greater than 475 °C [15, 16].

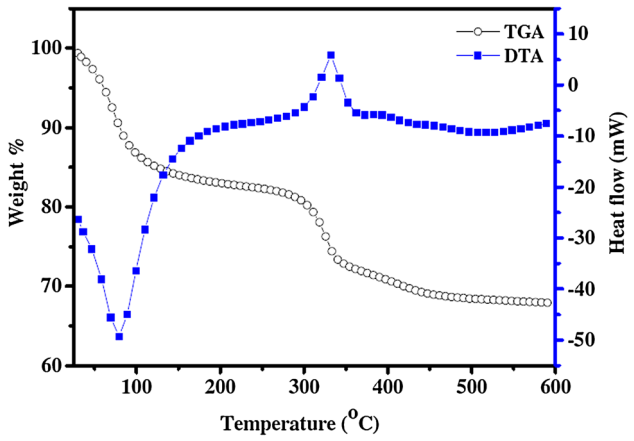

Fig. 1 TG–DTA curves of TiO_2 precursor prepared using 0.03 M of PVP

3.2 XRD studies

The XRD patterns of TiO_2 obtained by PTP using various amount of PVP as a capping agent at the calcination temperature of 500 °C are shown in Fig. 2. The mean crystallite size for the samples was calculated using Scherrer's formula [17]

$$D = \frac{0.91\lambda}{\beta \cos\theta}$$

where λ is the wavelength of the X-ray (1.5406 Å), β is the full width and half maximum of the diffracted peak, and θ is the diffracted angle. As-prepared sample did not have any peak during the X-ray diffraction that indicates its amorphous nature. The XRD pattern of the calcined samples was well indexed to the anatase phase, and the patterns were matched with JCPDS 84-1286 [18]. The nonappearance of diffraction peaks at 27° indicates that the prepared samples were free from the rutile structure of TiO_2. The peaks observed at 2θ angles of 25.23°, 36.89°, 37.81°, 38.60°, 48.07°, 53.85°, 55.08°, 62.77°, and 68.80°

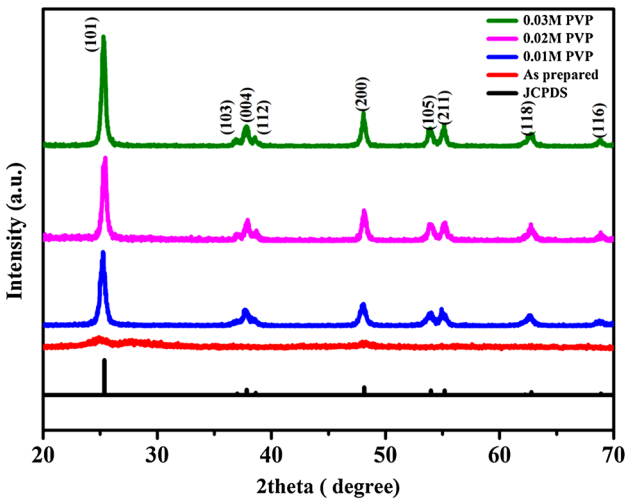

Fig. 2 XRD patterns of TiO_2 NPs prepared using various amounts of PVP

correspond to the (101), (103), (004), (112), (200), (105), (211), (118), and (116) planes, respectively. Therefore, the prepared TiO_2 has a highly crystalline anatase phase having a tetragonal structure [19]. The average crystallite size was measured from the most predominant XRD peak (101) at 25.23° using the above Scherrer's formula and found to be 22 nm. The crystallite size of TiO_2 prepared using 0.02 M PVP has near crystalline size with standard TiO_2 paste (*Dyesol Ltd.*) [20].

3.3 SEM studies

Figure 3 shows the surface morphology of TiO_2 NPs calcined at 500 °C. It can be seen that the samples which show the particles almost spherical in shape and its diameter were found to be <40 nm. The TiO_2 NPs prepared by using 0.01 and 0.03 M of PVP were agglomerated, and their average particles size was found to be ~35 and ~26 nm, respectively. But, TiO_2 synthesized by using 0.02 M PVP exhibits particle size of ~24 nm with no agglomeration.

3.4 BET surface area analysis

The specific surface area of prepared TiO_2 NPs using various amounts of PVP was examined by using N_2 adsorption isotherm. Figure 4 shows that a representative BET surface area analysis of TiO_2 NPs prepared by using 0.02 M PVP has the higher specific surface area than other two TiO_2 samples (Table 1). The BET results have good agreement with the SEM results. The TiO_2 photoanode fabricated using standard TiO_2 paste (*Dyesol Ltd.*) has the surface area of 72.9 m^2/g [21], which is slightly higher than the same fabricated using the formulated TiO_2 paste and it was found to be 60.19 m^2/g.

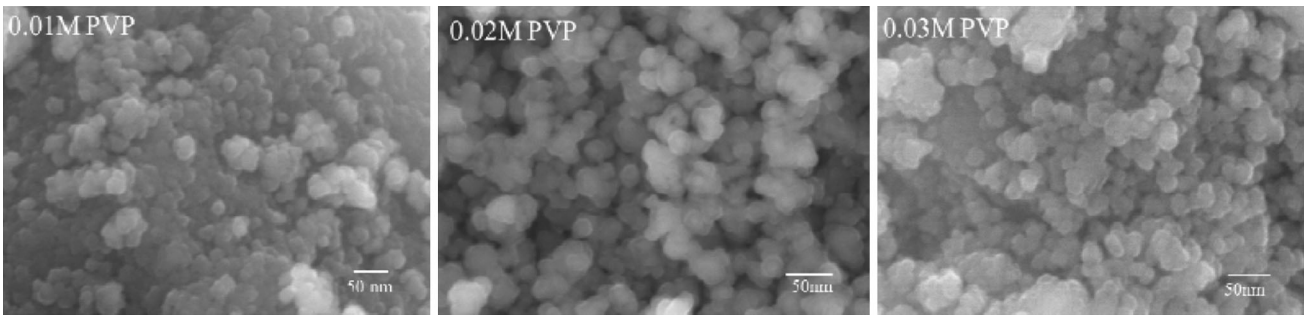

Fig. 3 SEM image of TiO_2 NPs synthesized using various amounts of PVP

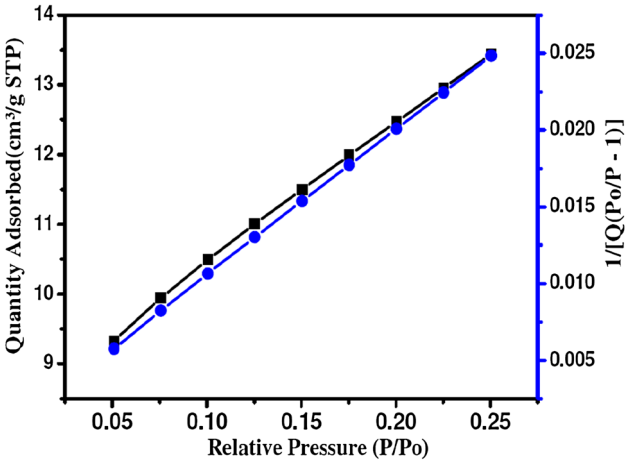

Fig. 4 BET surface area analysis for TiO_2 prepared using 0.02 M PVP

Table 1 BET surface area and particle size of TiO_2 NPs prepared by using various amounts of PVP

$TiCl_4$ (M)	PVP (M)	BET surface area (m^2/g)	Particle size (nm)
0.1	0.01	45.73	35
0.1	0.02	60.19	24
0.1	0.03	56.25	26

3.5 UV–Vis spectral studies

The absorption of TiO_2 NPs prepared by using 0.02 M PVP is shown in Fig. 5a. The maximum absorption is in the range of 200–400 nm [22]. The optical band gap of the material either direct or indirect is determined by using the formula related to absorption coefficient and is given below [23]

$$(\alpha h\nu)^m = h\nu - E_g$$

where α is the absorption coefficient, $h\nu$ is photon energy, and E_g is the band gap energy; m denotes the nature of the band gap either direct or indirect which has the value 2, ½ for direct and indirect band gap. The band gap calculated from the graph is plotted between $(\alpha h\nu)^2$ versus $h\nu$. Then, the value of E_g was determined by extrapolating the value of α to zero [24, 25]. The band gap of TiO_2 NPs prepared by using 0.02 M PVP was found to be 3.25 eV.

Figure 6 shows that the UV–Vis absorption spectra of N719 dye adsorbed the formulated TiO_2 paste and standard TiO_2 paste (*Dyesol Ltd.*)-based photoanode, respectively. The maximum dye adsorption was observed on both the films at 535 nm [26]. The formulated TiO_2 paste-based photoanode containing an optimized amount of 30 wt% prepared TiO_2 NPs, 15 wt% of ethyl cellulose, 50 wt% of terpineol, and 5 wt% of dibutyl phthalate only has very closer absorption intensity than the standard TiO_2 paste (*Dyesol Ltd.*)-based photoanode. This may be due to the lesser surface area of the formulated TiO_2 paste (60.19 m^2/g) than the standard TiO_2 paste (*Dyesol Ltd.*) (72.9 m^2/g; Table 2).

3.6 Photovoltaic performance studies

Figure 7 represents the photocurrent density–voltage (*J–V*) characteristics of DSSCs fabricated using the formulated TiO_2 and standard TiO_2 (*Dyesol Ltd.*) paste-based photoanodes at a light intensity of 100 mW/cm^2 under the standard global AM 1.5 irradiation, and their photovoltaic performance values are given in Table 3. It shows that the DSSC fabricated using the formulated TiO_2 paste-based photoanode has the efficiency of 4.5 % with a short-circuit photocurrent density (J_{sc}) of 9.6 mA/cm^2, open-circuit photovoltage (V_{oc}) of 0.70 V, and a fill factor (FF) of 67 %. But the DSSC fabricated using the standard TiO_2 paste (*Dyesol Ltd.*)-based photoanode has the cell efficiency of 4.6 % with a short-circuit photocurrent density (J_{sc}) of 9.8 mA/cm^2, open-circuit photovoltage (V_{oc}) of 0.69 V, and a FF of 68 %. DSSC fabricated using the formulated TiO_2 paste-based photoanode is slightly lesser PCE of 2.2 % than the same DSSC fabricated using standard TiO_2 (*Dyesol Ltd.*) paste-based photoanode. This is due to the slightly lesser surface area of the formulated TiO_2 paste-based photoanode than the standard TiO_2 NPs (*Dyesol Ltd.*)-based photoanode, and hence, the later has the

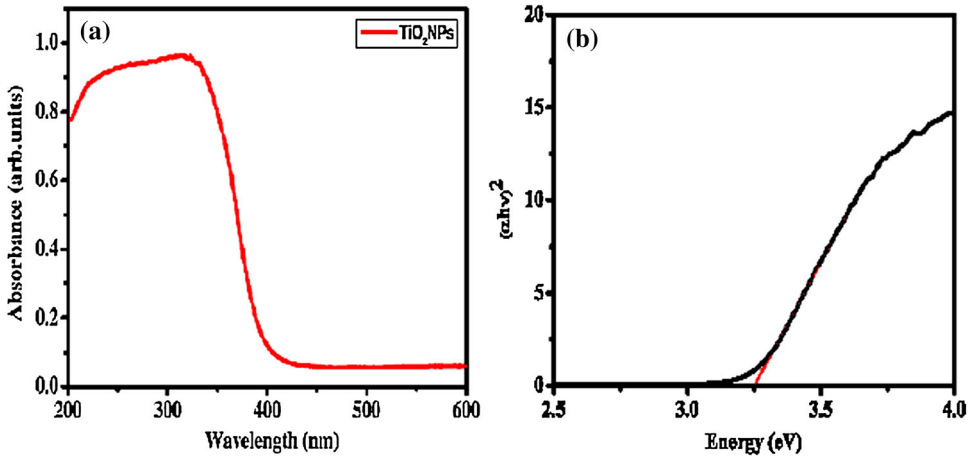

Fig. 5 **a** UV–Vis absorption spectrum of TiO_2 NPs prepared using 0.02 M of PVP and **b** a plot of $(\alpha h\nu)^2$ versus $h\nu$ of TiO_2 NPs prepared using 0.02 M of PVP

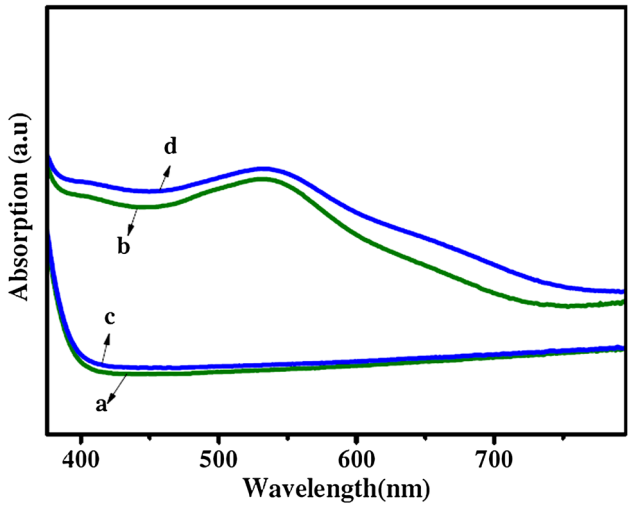

Fig. 6 Absorption spectra of N719 dye adsorbed on TiO_2 photoanodes; **a**, **b** before and after dye adsorption on formulated TiO_2 paste-based photoanode and **c**, **d** before and after dye adsorption on standard TiO_2 paste (*Dyesol Ltd.*)-based photoanode

Table 2 BET surface area and particle size of formulated TiO_2, standard TiO_2, and P25 TiO_2 pastes

Photoanode	BET surface area (m^2/g)	Particle size (nm)	Reference
Standard TiO_2 (*Dyesol Ltd.*) paste	72.90	20	[21]
P25 TiO_2 (*Degussa*) paste	50.00	30	[27]
Formulated TiO_2 paste	60.19	24	Present study

maximum adsorption of dye to get more number of electrons in the circuit. It is reported that the P25 TiO_2 (*Degussa*) paste-based photoanode has achieved PCE of 86.04 % with respect to DSSC fabricated using standard TiO_2 (*Dyesol Ltd.*) paste-based photoanode [27]. But, the

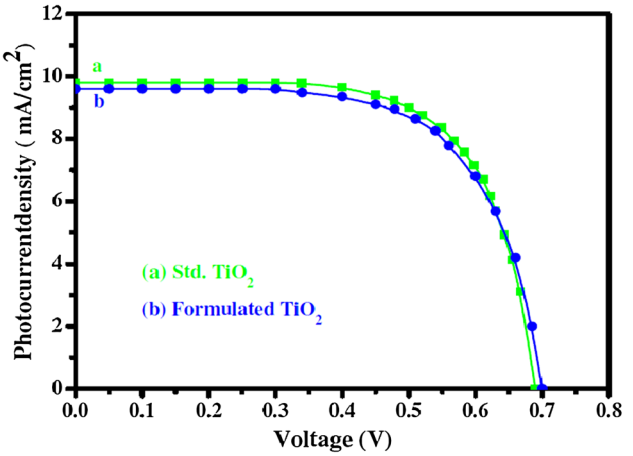

Fig. 7 J–V curves for DSSC fabricated using the formulated TiO_2 paste and standard TiO_2 paste-based photoanodes

DSSC fabricated using the formulated TiO_2 paste-based photoanode has achieved 97.83 % of PCE which is much higher than the same DSSC fabricated using P25 TiO_2 (*Degussa*) paste-based photoanode. This is due to lesser surface area of P25 TiO_2 (*Degussa*) paste than the formulated TiO_2 NPs paste (Table 2).

4 Conclusion

TiO_2 NPs were prepared by polyol thermolysis process using 0.02 M PVP as a capping agent. The average particles size of the prepared TiO_2 significantly depends on the amount of PVP. The thermal studies showed that the complete crystallization temperature of the prepared TiO_2 sample was found to be 500 °C. The phase purity of the prepared TiO_2 NPs was confirmed by XRD analysis. The band gap energy of TiO_2 NPs was found to be 3.25 eV. The photovoltaic performance of DSSC fabricated using the

Table 3 Comparison of photovoltaic parameters of DSSCs fabricated using the formulated TiO_2 paste, standard TiO_2 paste, and P25 TiO_2 paste-based photoanodes

Photoanode	J_{sc} (mA/cm^2)	V_{oc} (V)	FF	η (%)	Achieved PCE (%) w.r.t Standard TiO_2	Reference
Formulated TiO_2	9.6	0.70	0.67	4.50	97.83	Present study
Standard TiO_2 ((*Dyesol Ltd.*)	9.8	0.69	0.68	4.60	100.00	Present study
P25 TiO_2	8.5	0.70	0.70	4.13	86.04	[27]
Standard TiO_2 (*Dyesol Ltd.*)	10.7	0.69	0.65	4.80	100.00	[27]

formulated TiO_2 paste-based photoanode is nearly closer to that of the same DSSC fabricated using both the standard TiO_2 paste (*Dyesol Ltd.*) and much higher than the P25 TiO_2 (*Degussa*) paste-based photoanodes.

Acknowledgments One of the authors, Dr. A.S., gratefully acknowledges the Pondicherry University for providing the financial support under Start-up Research Project Grant (Ref.PU/PC/Startup/No. 19/2011-12) and the CIF of Pondicherry University for extending the instrumentation facilities.

References

1. S.-J. Lee, J. Choi, D.-W. Park, Mater. Sci. Eng., B **178**, 489 (2013)
2. S.N. Karthick, K.V. Hemalatha, C. Justin Raj, A. Subramania, H.-J. Kim, Thin Solid Films **520**, 7018 (2012)
3. C.J. Barbe, F. Arendse, P. Comte, M. Jirousek, F. Lenzmann, V. Shklover, M. Gratzel, J. Am. Ceram. Soc. **71**, 3157 (1997)
4. Y. Saito, S. Kambe, T. Kitamura, Y. Wada, S. Yanagida, Sol. Energy Mater. Sol. Cells **83**, 1 (2004)
5. A. Karami, J. Iran. Chem. Soc. **7**, 154 (2010)
6. D. Monti, A. Ponrouch, M. Estruga, M.R. Palacín, J.A. Ayllón, A. Roig, J. Mater. Res. **28**, 340 (2012)
7. S. Jeon, P.V. Braun, Chem. Mater. **15**, 1256 (2003)
8. S.N. Karthick, K. Prabakar, A. Subramania, J.-T. Hong, J.-J. Jang, H.-J. Kim, Powder Technol. **205**, 36 (2011)
9. J.W. Kang, D.H. Kim, V. Mathew, J.H. Gim, I. Yu, C.H. Woo, E.J. Kim, C.H. Choi, J.K. Kim, Defect Diffus Forum **312–315**, 160 (2011)
10. B.C. Feldmann, Adv. Funct. Mater. **13**, 101 (2003)
11. A. Subramania, G.V. Kumar, A.R.S. Priya, T. Vasudevan, Nanotechnology **18**, 225601 (2007)
12. S.K. Tripathy, T. Sahoo, M. Mohapatra, S. Anand, Y.-T. Yu, J. Phys. Chem. Solids **70**, 147 (2009)
13. Y. Yan, J. Wang, Q. Chang, M. Babikier, H. Wang, H. Li, Q. Yu, S. Gao, S. Jiao, Electrochim. Acta **94**, 277 (2013)
14. Z. Salam, E. Vijayakumar, A. Subramania, RSC Adv. **4**, 52871 (2014)
15. E.T. Acta, P. Jane, T. Yeh, Thermochim. Acta **297**, 85 (1997)
16. J. Zhu, J. Yang, Z.-F. Bian, J. Ren, Y.-M. Liu, Y. Cao, H.-X. Li, H.-Y. He, K.-N. Fan, Appl. Catal. B Environ. **76**, 82 (2007)
17. G.J. Wilson, A.S. Matijasevich, D.R.G. Mitchell, J.C. Schulz, G.D. Will, Langmuir **22**, 2016 (2006)
18. K. Thamaphat, P. Limsuwan, B. Ngotawornchai, Nat. Sci. **42**, 357 (2008)
19. I. Hernández, A.M. Maubert, L. Rendón, P. Santiago, H.H. Hernández, Int. J. Electrochem. Sci. **7**, 8832 (2012)
20. E.J.W. Crossland, N. Noel, V. Sivaram, T. Leijtens, J.A. Alexander-Webber, H.J. Snaith, Nature **495**, 215 (2013)
21. H. Wang, M. Liu, C. Yan, J. Bell, Beilstein J. Nanotechnol. **3**, 378 (2012)
22. K.M. Reddy, S.V. Manorama, A.R. Reddy, Mater. Chem. Phys. **78**, 239 (2002)
23. G.K. Mor, O.K. Varghese, M. Paulose, C.A. Grimes, Adv. Funct. Mater. **15**, 1291 (2005)
24. S. Mathew, A.K. Prasad, T. Benoy, P.P. Rakesh, M. Hari, T.M. Libish, P. Radhakrishnan, V.P.N. Nampoori, C.P.G. Vallabhan, J. Fluoresc. **22**, 1563 (2012)
25. N.S. Begum, H.M.F. Ahmed, Bull. Mater. Sci. **31**, 43 (2008)
26. S.N. Karthick, K.V. Hemalatha, C.J. Raj, H. Kim, M. Yi, J. Ceram. Process. Res. **13**, 136 (2012)
27. G.P. Demopoulos, C. Charbonneau, K.E. Lee, G.B. Shan, M.A. Gomez, R. Gauvin, ECS Trans. **21**, 23 (2009)